nature portfolio

https://doi.org/10.1038/s41551-021-00781-2

Supplementary information

Enhanced intratumoural activity of CAR T cells engineered to produce immunomodulators under photothermal control

In the format provided by the authors and unedited

Contents:

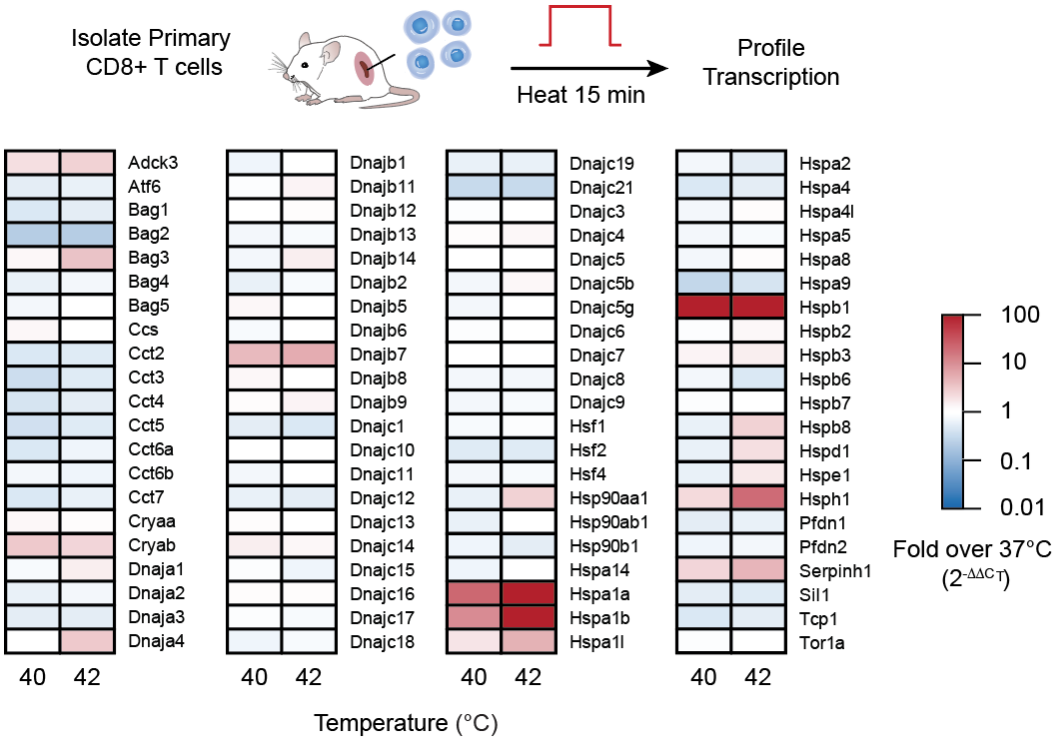

Supplementary Figure 1: qPCR screen of HSPs in primary murine T cells. Splenic CD8+ T cells were isolated using the CD8+ T cell isolation kit according to (Miltenyi 130-104-075). Six hours after indicated heat treatments, mRNA was harvested and quantified using the Mouse HSP profiler kit (Qiagen PAMM-076Z) according to manufacturer instructions. Data are displayed relative to unheated controls.

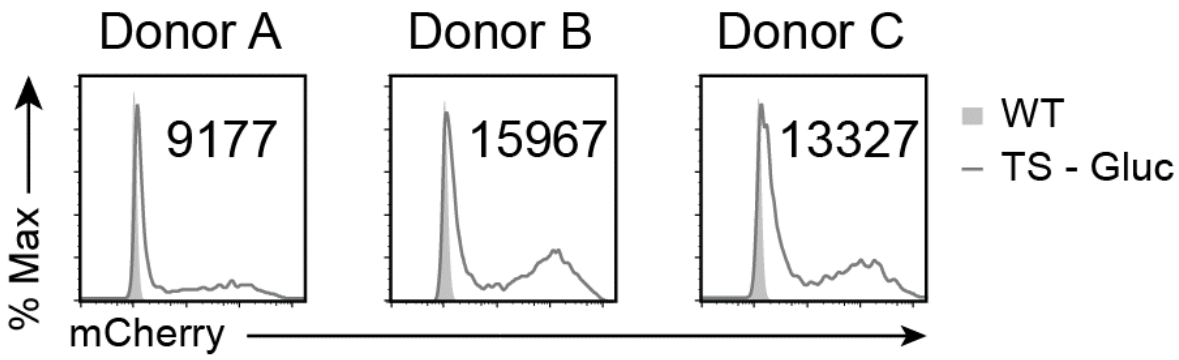

Supplementary Figure 2: Transduction efficiencies of primary human T cells from three donors. Flow cytometric plots of primary human T cells derived from 3 donors and transduced with the Gluc expressing 7H-YB Thermal switch containing a constitutively expressed mCherry reporter. Inset shows the mean fluorescent intensity (MFI) of mCherry transduced cells.

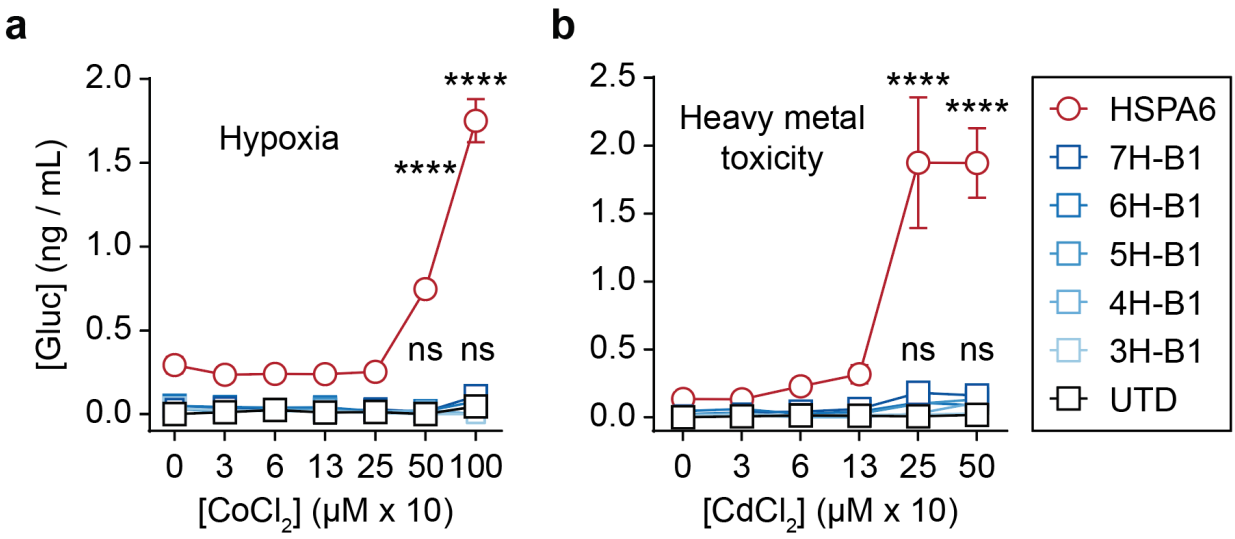

Supplementary Figure 3: Thermal switch specificity in Jurkat T cells. Gluc activity by Jurkat T cells transduced with synthetic thermal gene switch constructs (blue) or the endogenous HSPA6 promoter (red) following exposure to (**a**) $CoCl_2$ to mimic hypoxia or (**b**) to $CdCl_2$ to model heavy metal toxicity (ns = not significant, ****P<0.0001, two-way ANOVA and Tukey post-test and correction, error bars show SEM, n = 3).

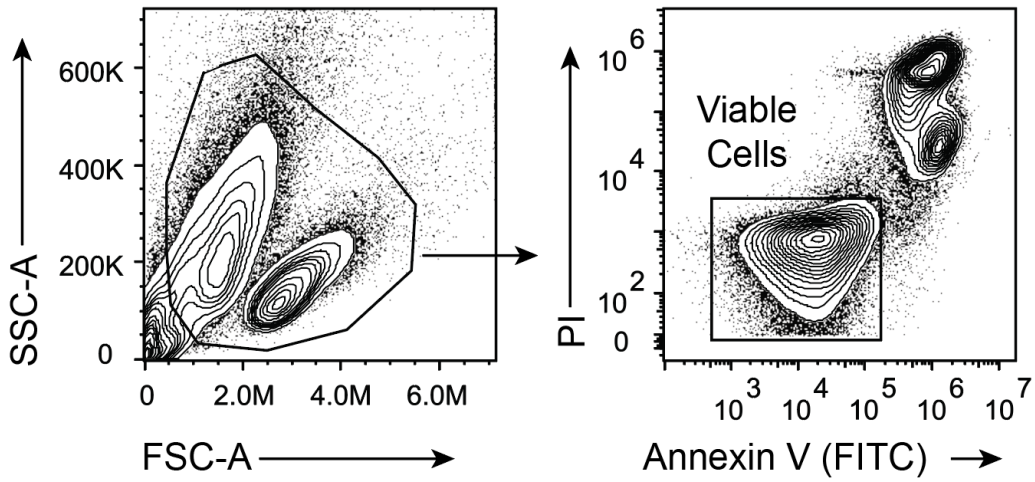

Supplementary Figure 4: Gating strategy for viability flow staining. Primary human T cells were heated at 42 °C for 60 minutes as a positive control for thermal damage. Shorter regimens were used for subsequent experiments. Because many of the AnnexinV+ or PI+ events were not within tighter FSC/SSC gates, this conservative gating strategy was used as it better represented the sample's overall viability.

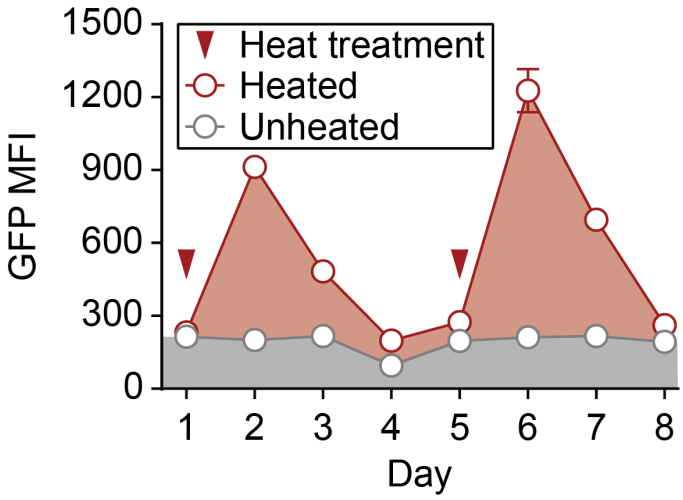

Supplementary Figure 5: Longitudinal heating of primary human T cells. Primary human T cells transduced with an HSPA6-GFP switch were repeatedly heated once GFP signal had returned to baseline after previous heat treatment (n = 3 biologically independent wells, error bars show SEM). Two independent experiments were performed with similar results.

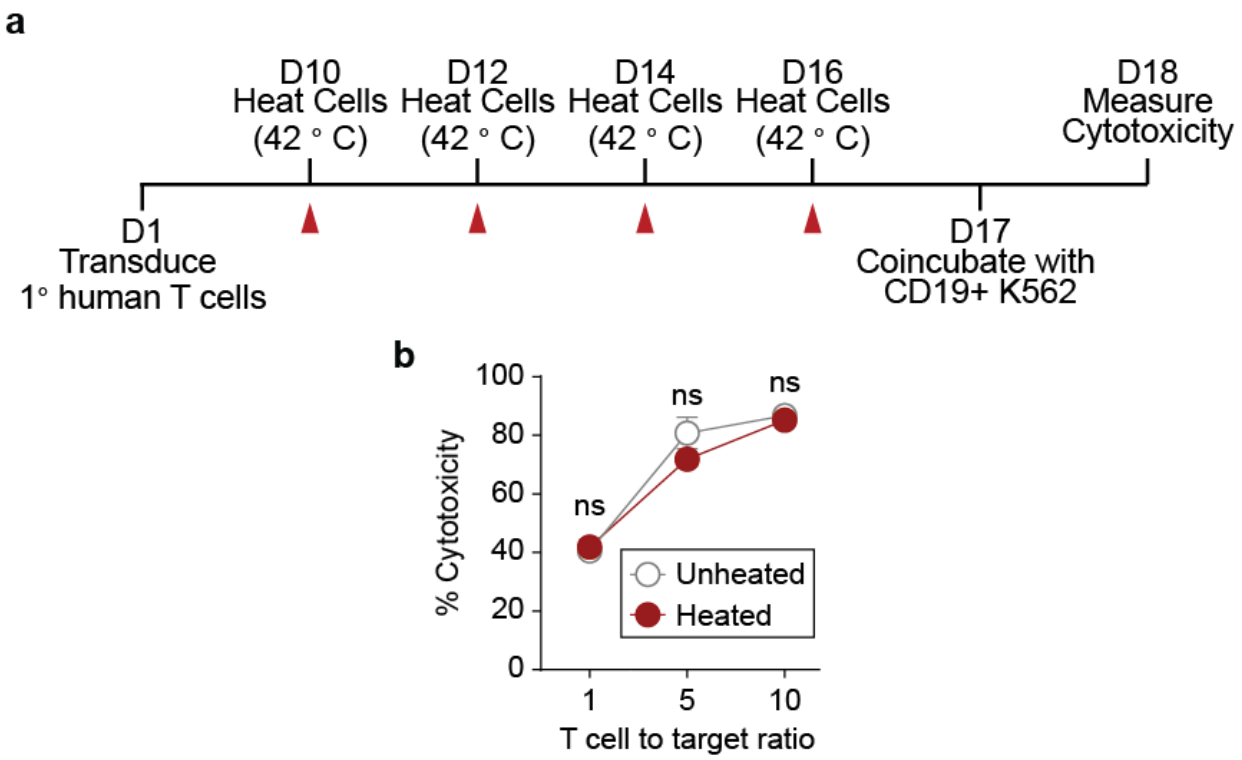

Supplementary Figure 6: Repeated heat treatments do not affect CAR T cell cytotoxicity. (**a**) Primary human T cells were transduced to constitutively express an αCD19 CAR following CD3/CD28 bead activation. Heat treatments were performed at indicated timepoints prior to coincubation with luciferized, CD19+ K562s according to the timeline. (**b**) Percent cytotoxicity was quantified by loss of luminescence in wells relative to control wells containing only target cells (b) (ns = not significant, two-way ANOVA and Sidak post-test and correction, mean ± SEM is depicted, n = 3 biologically independent wells).

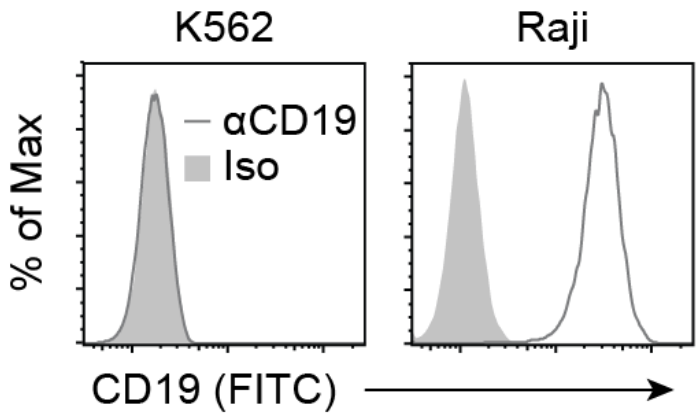

Supplementary Figure 7: CD19 expression on K562 and Raji tumour cells. Representative flow cytometric plots of CD19 staining on K562 and Raji cell lines (Iso = isotype control).

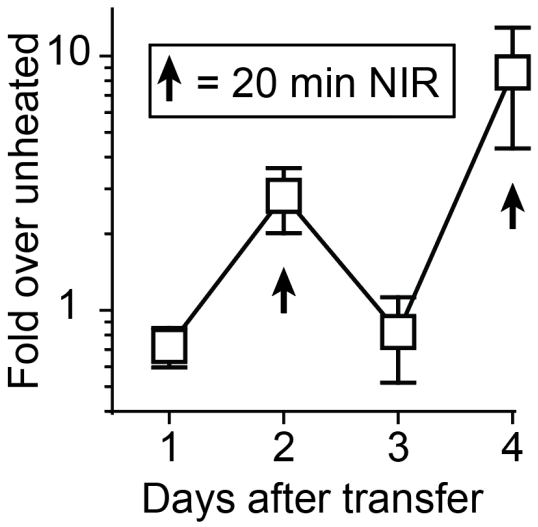

Supplementary Figure 8: Longitudinal control of intratumoural CAR T cells using photothermal pulses. Mice bearing Raji tumours (CD19+) were injected i.v. with TS-Fluc T cells. Tumour sites were irradiated on days 2 and 4 using NIR laser light as shown in **Figure 5d**. Luminescence was quantified daily via i.v. injections of D-luciferin (n = 3, biologically independent wells, error bars show SEM).

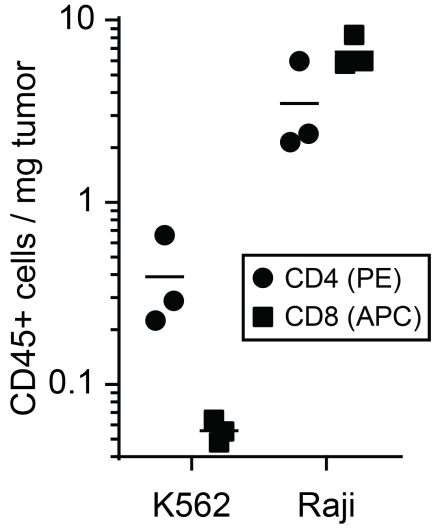

Supplementary Figure 9: TS-Fluc αCD19 CAR T cell infiltration into K562 and Raji flank tumours. TS-Fluc αCD19 CAR T cells were injected i.v. into tumour bearing mice once tumours had reached ~250 mm^3. After 7 days, tumours were resected, dissociated, and stained to quantify cellular infiltration using flow cytometry counting beads (n = 3, biologically independent wells, error bars show SEM).

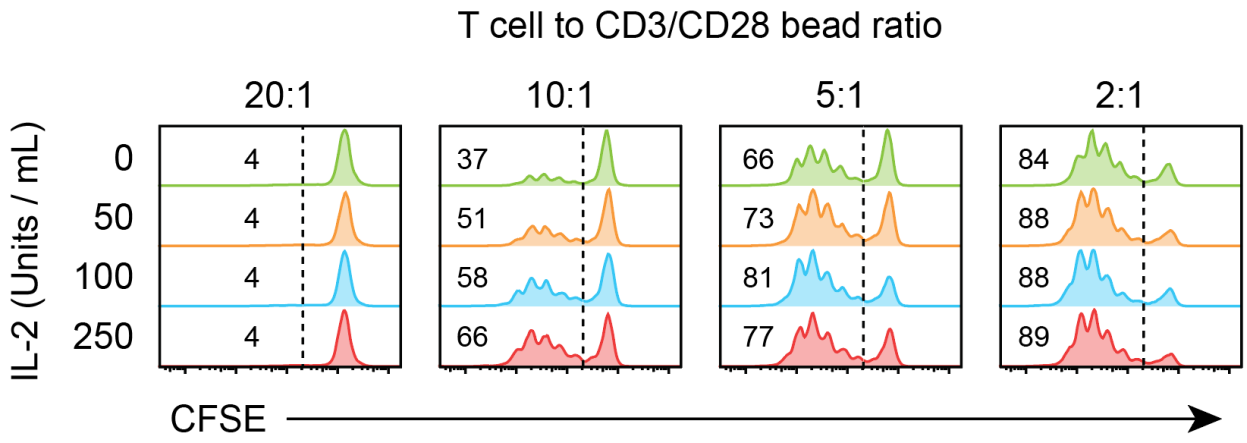

Supplementary Figure 10: Cytokine support improves proliferation of T cells receiving low levels of CD3/28 stimulation. T cells were labeled with CFSE and incubated with low levels of activating beads. For reference, routine expansion and culture of T cells uses 3 beads for every T cell. Increasing amounts of IL-2 were added to each bead ratio. All samples were assayed after 4 day incubations at indicated conditions. Two independent experiments were performed with similar results.

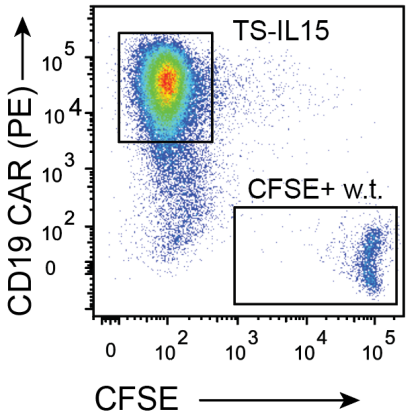

Supplementary Figure 11: Gating strategy for mixed proliferation experiment. Transduced TS-15 αCD19 CAR T cells were identified by CAR expression. Proliferation of CFSE+ wild-type cells was assessed by dye dilution and FlowJo proliferation tool.

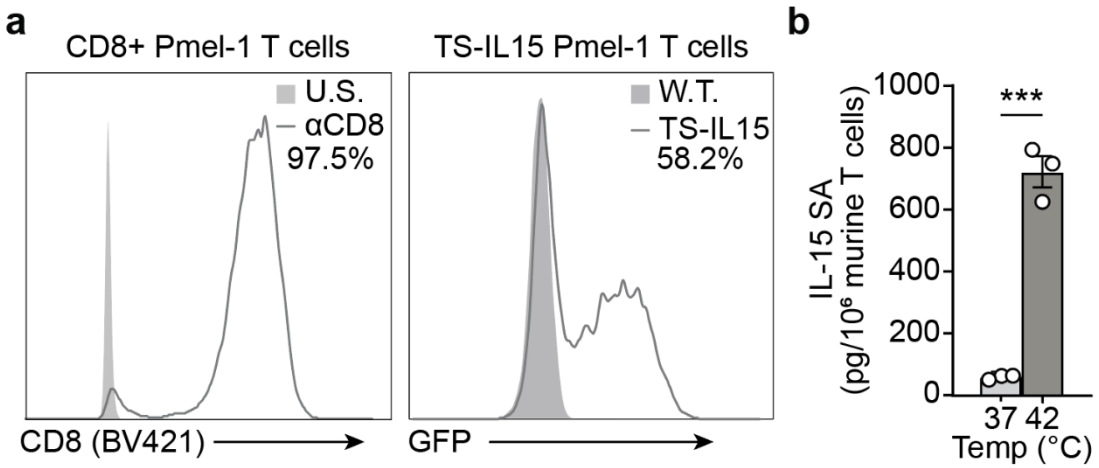

Supplementary Figure 12: Characterization of engineered Pmel-1 T cells. 48 hours post isolation and peptide activation, Pmel-1 derived splenocytes were transduced with the TS-IL15 vector containing a constitutive GFP reporter. (**a**) Pmel-1 T cells were characterized via flow cytometry before adoptive transfer to assess CD8+ cell purity expansion (left) and transduction efficiency (right) (U.S. = Unstained Pmel-1 T cells, W.T = Wild type Pmel-1 T cells). (**b**) IL-15 production measured via ELISA from transduced murine T cells after 20 minute heating at indicated temperatures (*** P=0.0002, unpaired T test, mean± SEM is depicted, n = 3 biologically independent wells).

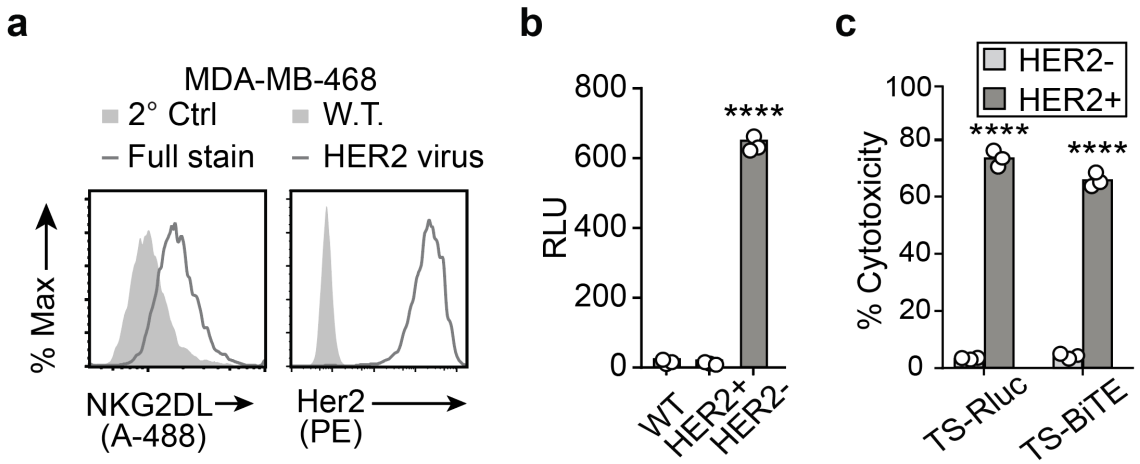

Supplementary Figure 13: Validation of MDA-MB-468 transduced with HER2 or Renilla Luciferase. (**a**) Representative flow plots of NKG2DL staining and HER2 Staining of HER2+ MDA-MB-468s. MDA-MB-468 were transduced with lentivirus to stably surface express HER2. (**b**) Luminescence of Fluc transduced HER2- MDA-MB-468 tumour cells (**** P<0.0001, one-way ANOVA and Sidak post-test and correction, mean ± SEM is depicted, n = 3 biologically independent wells). (**c**) Percent cytotoxicity observed via LDH assay in HER2- or HER2+ MDA-MB-468 cells after incubation with T cells constitutively expressing CARs (****P<0.0001 between HER2- and HER2+ groups, two-way ANOVA and Sidak post-test correction, mean ± SEM is depicted, n = 3 biologically independent wells). Two independent experiments were performed with similar results.

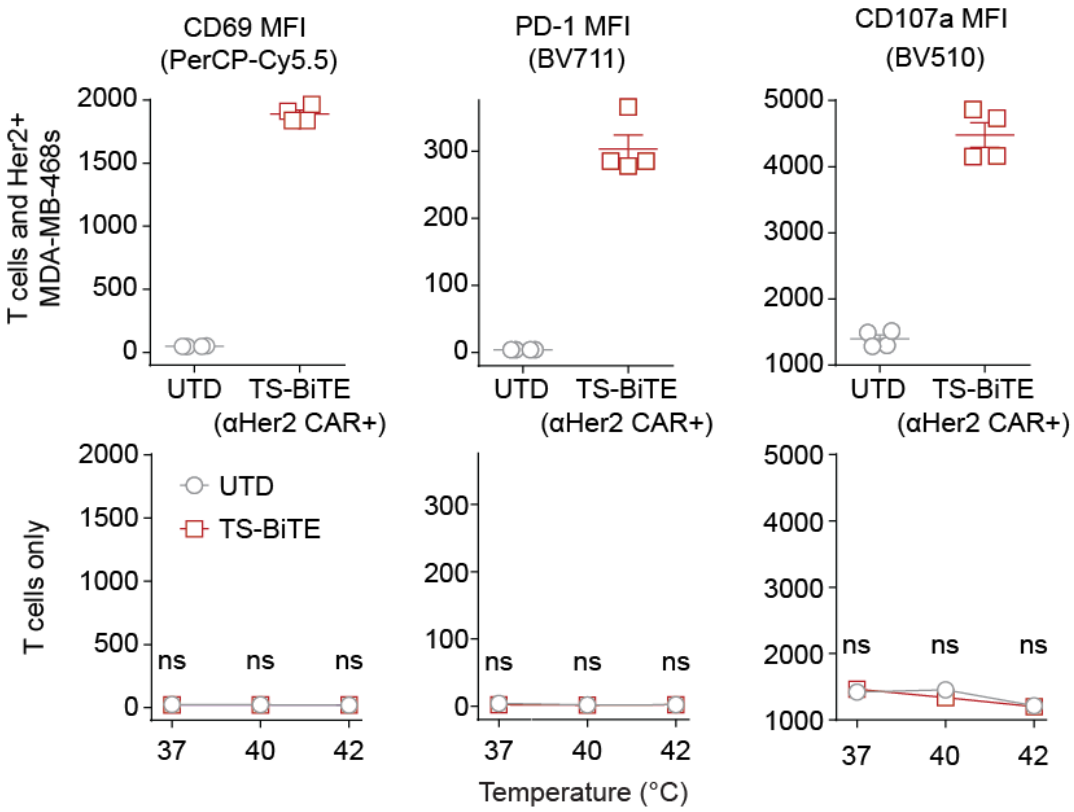

Supplementary Figure 14: TS-BiTE αHER2 CAR T cells activate when incubated with HER2+ MDA-MB-468 cells. MFIs of activation and degranulation markers CD69, PD-1, and CD107a on TS-BiTE αHER2 CAR T cells that were heated at indicated temperatures prior to co-incubation with HER2+ MDA-MB-468 target cells. (ns = not significant, two-way ANOVA and Tukey post-test and correction, error bars show SEM, n = 4 biologically independent wells).

Genetic Locus	Jurkat E6.1	K-562	MDA-MB-468	Raji
D3S1358	15, 17	16	15	15, 16
TH01	6, 9.3	9.3	7	6, 7
D21S11	31.2, 32.2, 33.2, 34.2	29, 30, 31	27, 28	28, 31
D18S51	13, 20, 21	15, 16	17	17
Penta E	10, 12	5, 14	5	5, 13
D5S818	9	11, 12	12	10, 13
D13S317	8, 12	8	12	13
D7S820	8, 12, 13	9, 11	8	10
D16S539	11	11, 12	9	8, 11
CSF1PO	10, 11, 12, 13	9, 10	12	10, 12
Penta D	11, 13	9, 13	8, 10	3.2, 9
vWA	18, 19	16	18	16, 19
D8S1179	13, 14, 15	12	13	14, 15
TPOX	8, 10	8, 9	8, 9	8, 13
FGA	20, 21	21	23	19, 27
AMEL	X, Y	X	X	X, Y
Mouse Contamination	Not detected	Not Detected	Not Detected	Not Detected
% Match	**91.89%**	**100%**	**100%**	**100%**

Supplementary Table 1: Cell line authentication via STR analysis. Jurkat E6.1, K-562, MDA-MB-468, and Raji human cell lines were authenticated via PowerPlex16HS STR profiling (Labcorp). Results were compared to known samples in the Cellosaurus STR Similarity Search Tool (CLASTR 1.4.4) database.